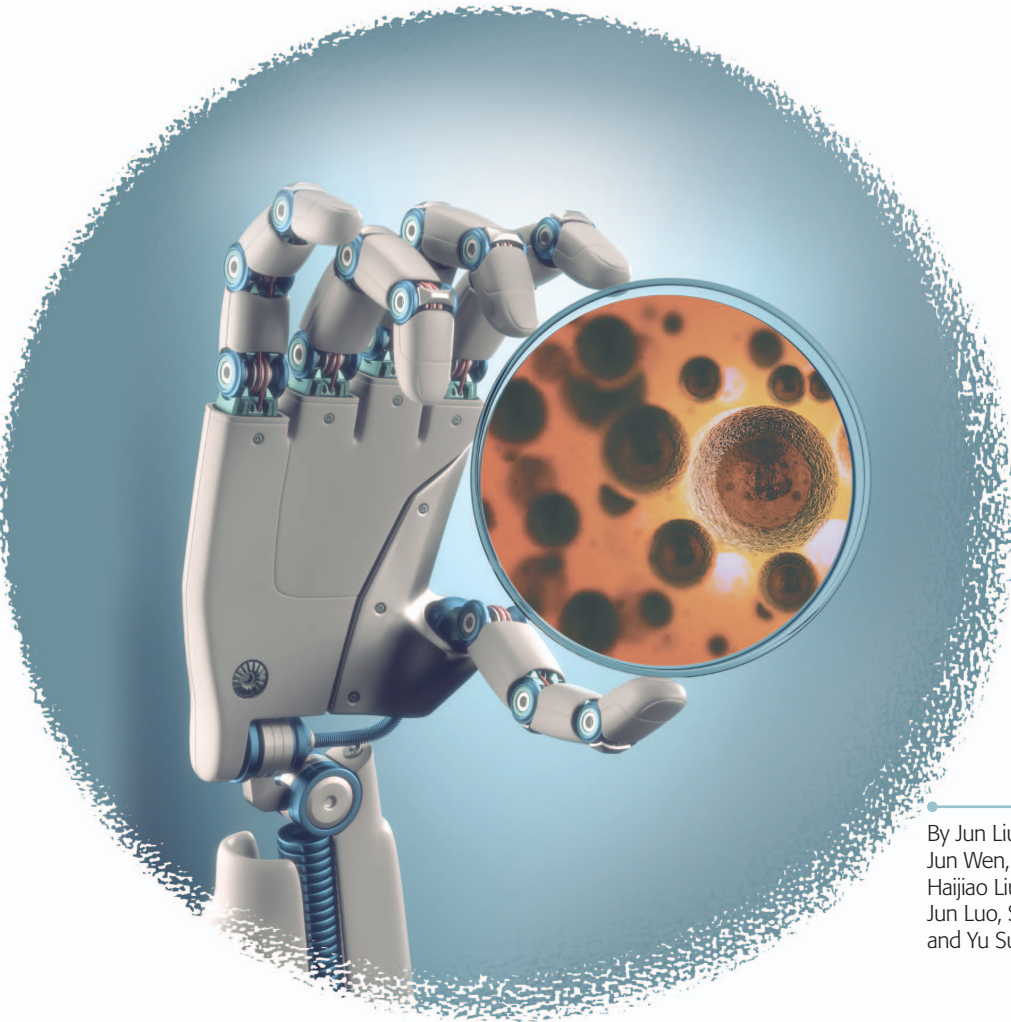


© ISTOCKPHOTO.COM/KTSIMAGE,  
CELLS—© ISTOCKPHOTO.COM/ROYALTYSTOCKPHOTO



By Jun Liu, Chaoyang Shi,  
Jun Wen, Derek Pyne,  
Haijiao Liu, Changhai Ru,  
Jun Luo, Shaorong Xie,  
and Yu Sun

# Automated Vitrification of Embryos

**T**his article reports on the first robotic system for vitrification of mammalian embryos. Vitrification is a technique used for preserving oocytes and embryos in clinical in vitro fertilization (IVF). The procedure involves multiple steps of stringently timed pick-and-place operation for processing an oocyte/embryo in vitrification media. In IVF clinics, the vitrification is conducted manually by highly skilled embryologists. Processing one oocyte/embryo takes the embryologist 15–20 min, depending on the protocols chosen to implement. Due to poor reproducibility and inconsistency across operators, the success and survival rates also vary significantly. Through collaboration with

IVF clinics, we are in the process of realizing robotic vitrification (RoboVetri) and ultimately aim to standardize clinical vitrification from manual operation to fully automated robotic operation. Our robotic system is embedded with two contact detection methods to determine the relative  $z$  positions of the vitrification micropipette, embryo, and vitrification straw. A three-dimensional (3-D) tracking algorithm is developed for visually served embryo transfer and real-time monitoring of embryo volume changes during vitrification. The excess medium is automatically removed from around the vitrified embryo on the vitrification straw to achieve a high cooling rate.

Tests on mouse embryos demonstrate that the system is capable of performing vitrification with a throughput at least three times that of manual operation and a high survival (88.9%) and development rate (93.8%).

Digital Object Identifier 10.1109/MRA.2014.2386195  
Date of publication: 23 March 2015

## Cryopreservation

Cryopreservation of mammalian reproductive cells is an essential technique in IVF clinics [1]. Oocytes and embryos are routinely frozen and cryopreserved. Patients who undergo therapeutic procedures (e.g., chemotherapy) that can place their fertility at risk have the option of preserving their oocytes for use at a later time through IVF techniques. Moreover, fertilized embryos are often needed for more than one cycle of IVF treatment. The rest of the fertilized embryos are cryopreserved for future use [2].

The techniques of oocyte/embryo cryopreservation are classified into two categories: 1) slow freezing and 2) fast freezing (i.e., vitrification) [3]. Vitrification, or fast freezing, is proven to be the more effective method and was first reported in [4]. Vitrification is superior to slow freezing [5] because it vitrifies the oocyte/embryo with no ice crystal formation during freezing, resulting in higher cell survival rates. The addition of cryoprotectants in vitrification increases embryo viscosity and makes the vitrified embryos syrupy. When the vitrified oocytes/embryos are placed in liquid nitrogen, the syrupy content inside the cell forms amorphous ice instead of ice crystals, which minimizes the vital damage to the cell during freezing [6].

At present, oocyte/embryo vitrification is done manually in IVF clinics globally. An operator looks through the microscope eyepieces and manipulates oocytes/embryos using a micropipette. An oocyte/embryo is first picked up and removed from the culture dish and washed with the equilibrium solution (ES) and a series of vitrification solutions (VSs), as shown in Figure 1. Within each step, timing control has been proven critical. After the many pick-and-place steps, the processed oocyte/embryo is placed onto a device called a *vitrification straw*. The volume of solution remaining around the oocyte/embryo on the straw must be minimal to ensure a high cooling rate [7]. The vitrification straw is then plunged into liquid nitrogen for freezing and long-term cryopreservation. Several commercial the VSs and protocols exist; however, their core steps are largely the same. All the protocols involve multiple washing steps with the ES and the VS, placing the vitrified oocytes/embryos on vitrification straws, and freezing the vitrification straws in liquid nitrogen. Manual oocyte/embryo vitrification is a laborious and demanding task due to the following reasons.

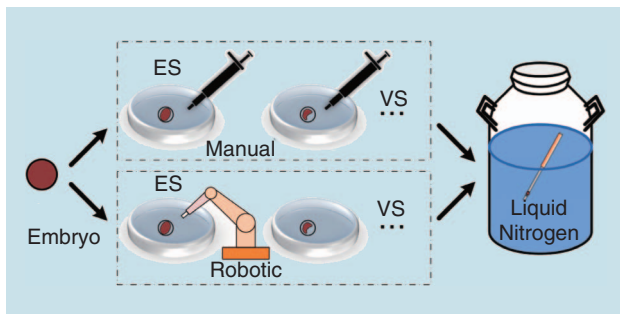


**Figure 1.** The schematic showing the manual and RoboVetri approaches. Vitrification involves multiple steps of cell pick and place before freezing in liquid nitrogen.

- There is a long learning curve, and intense focus is required for embryologists performing the manual method.
- The antifreezing solutes [e.g., dimethyl sulfoxide (DMSO)] are toxic to oocytes/embryos. Therefore, the washing time in the VS is critical but can be difficult to strictly control by an operator.
- Because of their small size ( $\sim 100\ \mu\text{m}$ ), oocytes/embryos can be difficult to detect and manipulate, especially when the medium surrounding the cells is dynamically changing (e.g., in viscosity) during micropipette aspiration and dispensing.
- The manual process has stringent skill requirements, and the success rate and cell survival rate can vary significantly across operators.

Over the past few decades, the robotics community has made significant progress in assisting/standardizing clinical procedures, from the transformative da Vinci surgical system to robotic systems under intensive development for manipulating single cells [8], [11]. To realize RoboVetri for clinical use, a number of tasks must be tackled with clinically acceptable reliability, for instance, robust embryo tracking in three dimensions in media of different viscosities and autonomous transfer of processed embryos from liquid environments to the solid vitrification straw tip. Furthermore, timing control in vitrification is much more stringent and critical than other cell manipulation tasks (e.g., intracytoplasmic sperm injection [12]) to achieve high cell development rates after embryo thawing.

Although automated vitrification was attempted using microfluidic approaches [13], [14], embryo loss is a concern because of difficulties in loading and retrieving embryos onto and from the microfluidic devices. No attempt has been made to automate vitrification using a robotic approach.

In this article, we present a robotic system prototype for automated vitrification and thawing of embryos. The system has successfully addressed the major challenges in manual operation with the following technologies: 1) automated locating of micropipette and vitrification straws, 2) contact detection methods to determine the relative  $z$  position of the micropipette tip, 3) autonomous detection and tracking of embryos in three dimensions, and 4) robotically placing vitrified embryos onto vitrification straws and removing excess medium. These core techniques make it practical to perform automated RoboVetri of embryos. The experimental results also demonstrate that the embryo survival and development rates after vitrification and thawing achieved by the robotic system were higher than those of the manual group. Automated vitrification would free up embryologists to focus on other tasks in IVF clinics and provide consistently high success and survival rates. With a higher throughput, automated vitrification also has the potential to become a standard tool for assessing existing vitrification protocols and developing new protocols.

## System Overview

As shown in Figure 2(a), the RoboVetri system is built around a standard upright microscope (Olympus SZX16, Olympus Canada, Inc.) that is equipped with motorized magnification control and motorized focusing. Mounted on the microscope is an

XY-motorized stage (ProScan, Prior Scientific, Inc.), which has a travel range of 75 mm and a resolution of 0.01  $\mu\text{m}$  along both axes. A custom-designed carrier plate [Figure 2(a) inset] is placed on the XY stage to hold an embryo culture dish, a multiwell plate, and multiple vitrification straws. A three-degree-of-freedom robot (MP285, Sutter, Inc.) carrying a vitrification micropipette (tip diameter: 150  $\mu\text{m}$ ) is used to manipulate embryos. A 25- $\mu\text{L}$  glass syringe (Hamilton Company) is mounted on a linear stage (eTrack, Newmark System, Inc.) for controlled aspiration and dispensing of embryos into or out of the vitrification micropipette. A camera (scA1300-32gm, Basler, Inc.) is connected to the microscope to provide visual feedback. A host computer controls all hardware via our custom-developed control software.

The robotic micromanipulator and XY stage are cooperatively controlled for positioning the vitrification micropipette along the  $xyz$  axes and positioning embryos in the  $xy$  plane, respectively. The overall control architecture of the automated system is summarized in Figure 2(b). The techniques for micropipette tip detection and embryo tracking are described in the “Contact Detection” and “3-D Embryo Tracking” sections, which provide position feedback to position the micromanipulator and the XY stage, forming an image-based visual servo control system.

In RoboVetri, the system first performs an autolocating of the end effector, a technique we previously reported in [15], for the robotic system to automatically detect the micropipette tip. Two contact detection methods are used by the system to determine the relative  $z$  position of the micropipette tip to the multiwell plate bottoms and the vitrification straw tip. During the washing steps, a 3-D tracking algorithm integrated with a Kalman filter is used to track the embryos. After washing in the ES and the VS, the robotic system automatically transfers the vitrified embryo out of the liquid environment onto the vitrification straw tip and removes the excess medium to realize the minimum volume requirement in vitrification. The vitrification straw carrying a vitrified embryo is placed in liquid nitrogen. Similar to the

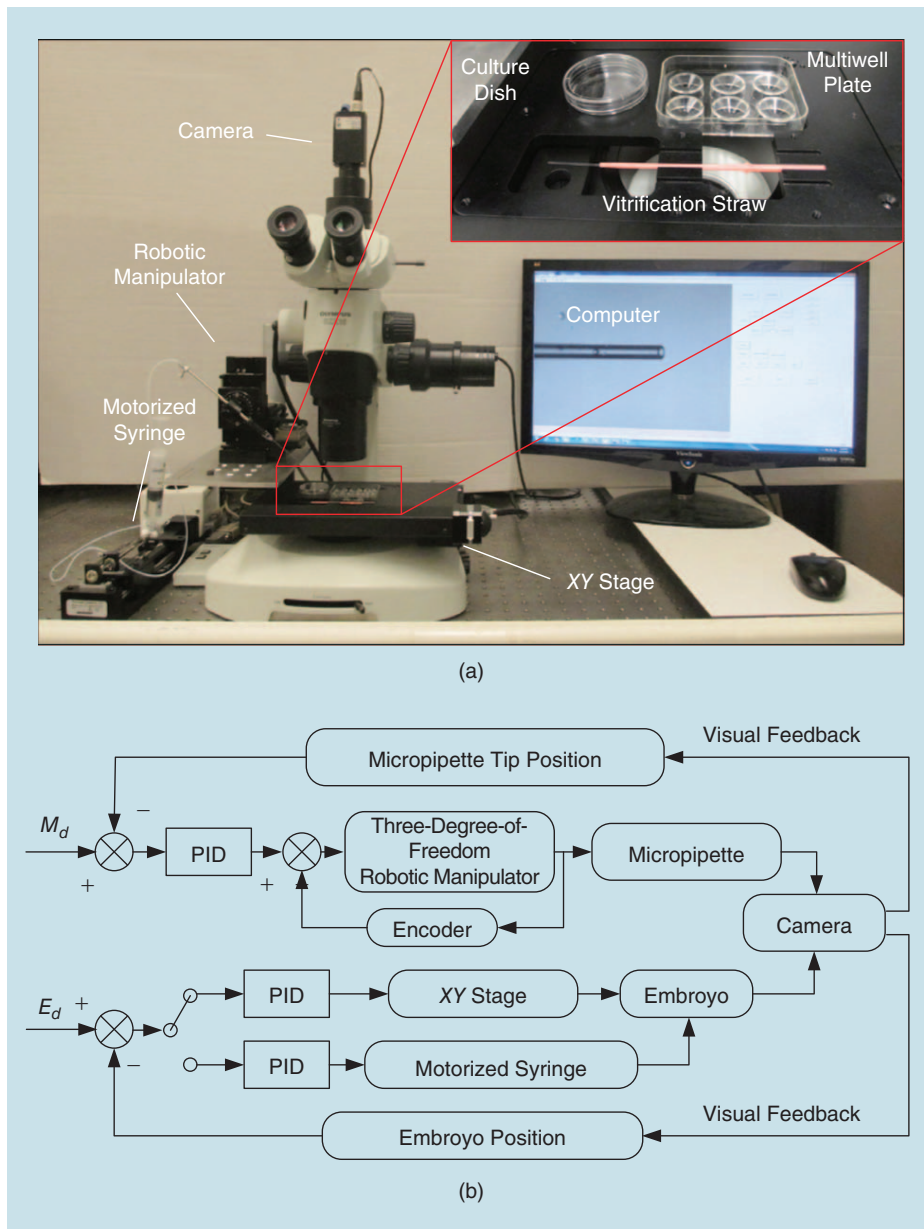


**Figure 2.** (a) The RoboVetri system prototype. The inset is the custom-designed carrier plate. (b) The system control architecture.

vitrification process, the frozen embryos are thawed and the system performance is evaluated by quantifying the post-thaw cell survival and development rate.

## Key Methods

### Contact Detection

Optical microscopy has a limited depth of field, making position detection along the  $z$  axis difficult. The relative  $z$  distance between the micropipette tip and the embryos must be accurately determined before cell manipulation can start. Since the embryos are always placed on the bottom of a multiwell plate or on the surface of the vitrification straw tip, the system determines the relative  $z$  position of the micropipette tip by detecting its contact with the multiwell plate substrate and the straw surface.

During contact detection on the multiwell plate substrate, the system moves the micropipette tip downward to approach the plate substrate [Figure 3(a) and (c)]. When the micropipette tip contacts the plate bottom [Figure 3(a) and (e)], further downward movement induces the tip's horizontal sliding motion on the plate substrate, which changes the tip's position in the  $xy$  plane and the imaging plane. The system detects the initial  $xy$  position change and, thus, determines the initial contact of the vitrification micropipette tip with the plate substrate.

The detection of the micropipette tip contact on the vitrification straw surface is different from contact detection with the multiwell plate bottom. Vitrification straw tips are cantilevers in structure and have low stiffness compared with plate substrates. Therefore, instead of sliding on the soft vitrification straw surface, the micropipette tip's further downward motion after initial contact deflects the soft straw tip [Figure 3(b)]. When the straw is deflected by the micropipette tip, it becomes out of focus in imaging [Figure 3(f)]. Based on the computed focus measure [see (1) in the "3-D Embryo Tracking" section], the robotic system detects the contact between the micropipette tip and the straw tip surface. This contact detection step is critical before the robotic system can place the vitrified embryo onto the straw tip, which will be discussed in the "Placing Embryo on Vitrification Straw" section.

### 3-D Embryo Tracking

The system, after detecting the micropipette tip positions along the  $xyz$  axes relative to the embryos, performs embryo pick and

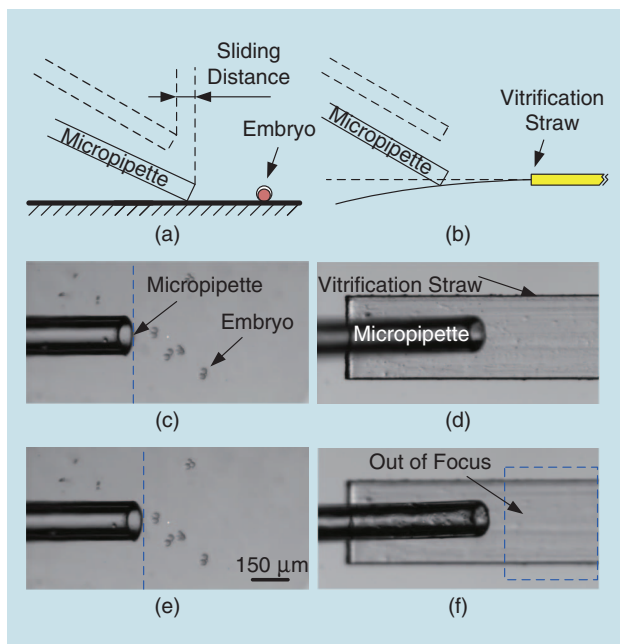


**Figure 3.** The detection of contact between the micropipette tip and the multiwell plate substrate and contact between micropipette tip and vitrification straw surface. (a) and (b) The schematic of contact detection on the plate substrate and vitrification straw, respectively. (c) and (d) The system moves the micropipette downward. (e) A further downward movement after contact induces the micropipette tip's sliding motion on the plate substrate surface. (f) A further downward movement after contact deflects the vitrification straw tip, causing it to become out of focus.

place to transfer the embryo from one type of solution to another (e.g., from the ES to the VS) via controlled micropipette aspiration. Due to the changes of fluid density and osmolarity, the embryo volume changes in the VS, resulting in variations of buoyancy. In addition, the fluidic flow from the micropipette dispensing also influences the embryo's positions. Thus, the embryos move dynamically in 3-D space when transferred into a different VS. To avoid losing the embryo and to enable efficient pick and place for ensuring stringent time control in each type of cryoprotectants, the robotic system must be able to robustly detect and track embryos three dimensionally.

When an embryo is dispensed out of the micropipette, a region of interest (ROI) is extracted at the micropipette tip [Figure 4(a)]. The ROI is denoised through the Gaussian smoothing method and binarized by applying Otsu's adaptive thresholding. A morphological close operation is then performed to remove noise and small particles that may be present in the ROI. In the binarized image, the contour of the detected foreground object is computed. The embryo's position in the image plane is detected by calculating the moment of the contour (see Figure 4, right column). The ROI is then updated to be centered at the embryo's centroid. The area of the embryo contour is also measured to reflect the embryo's volume change. For subsequent frames of images, the system repeats the execution of the process to track the embryo's position in the image plane (i.e., the  $xy$  plane).

To track the embryo's floating motion along the  $z$  axis, the system performs autofocus. The normalized variance method is used to calculate the focus measure. This method is chosen because it can effectively compensate for differences in the average image intensity ( $\mu$ ) by normalizing the final output with the mean intensity. The focus measure  $F$  changes as the embryo moves in the  $z$  direction inside the VS solution. As the focal plane moves close to the embryo, the contents in the image increase, causing the focus measure to increase. The system adjusts the microscope's focal plane according to maximizing the focus measure, and the position recorded by the

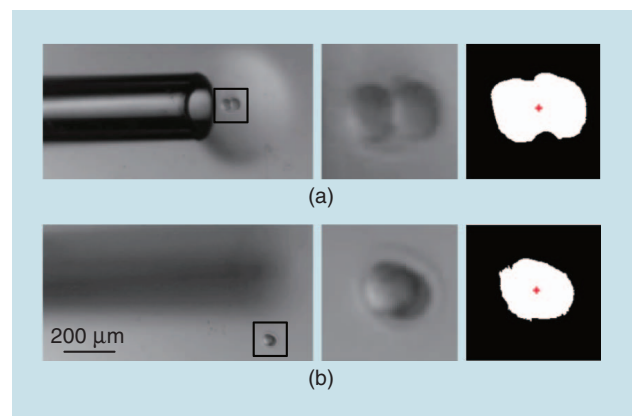


**Figure 4.** Embryo tracking in the VS. Left column: the original images with embryos at different heights. Middle column: the ROIs containing the tracked embryo target. Right column: the tracked embryo locations indicated by a red dot in the binarized image. (a) An embryo is dispensed out of micropipette into the VS solution. (b) An embryo is floating upward, due to buoyancy, whereas the system performs autofocus to control focus positions.

encoder of the focusing motor on the microscope is taken by the system to be the detected  $z$  positions

$$F = \frac{1}{H \cdot W \cdot \mu} \sum_H \sum_W (I(x,y) - \mu)^2, \quad (1)$$

where  $W$  and  $H$  are the ROI image width and height, respectively,  $I(x,y)$  is the pixel intensity at point  $(x,y)$ , and  $\mu$  is the average pixel intensity in the ROI.

The tracked embryo positions from autofocusing can be inaccurate due to the delay of changing the focal plane. Therefore, a Kalman filter is applied to correct the detected embryo positions. The embryo movement along the  $z$  direction is mainly caused by the dynamic change in buoyancy. The dynamics of the embryo's floating motion in the VSs is

$$\rho g V(t) - mg = m\ddot{x} + c\dot{x}, \quad (2)$$

where  $\rho$  is the liquid density,  $g$  is the gravitational acceleration,  $m$  is the mass of the embryo,  $x$  is the embryo's position along the  $z$  axis, and  $c$  is the damping ratio of the liquid. Due to osmotic stress in the VSs, the embryo volume  $V(t)$  changes over time [16]. The cell volume change in the VSs can be modeled as

$$\frac{dV(t)}{dt} = -L_p \cdot A \cdot R \cdot T \cdot \left( M_s + M_n - \frac{n_s}{V_w} - \frac{n_n}{V_w} \right) \quad (3)$$

$$\frac{dn_s}{dt} = P_D \cdot A \cdot \left( M_s - \frac{n_s}{V(t)} \right). \quad (4)$$

In this model, (3) describes the change of cell volume  $V(t)$  over time as a function of the hydraulic conductivity  $L_p$ , surface area  $A$ , gas constant  $R$ , temperature  $T$ , intracellular permeating  $M_s$ , and nonpermeating  $M_n$  solute concentration in the osmoles, and the extracellular permeating  $n_s$  and nonpermeating  $n_n$  solute concentration. Equation (4) describes the change in the intracellular moles of permeating solute  $n_s$  over time as a function of the DMSO permeability  $P_D$ . When substituting  $V(t)$  into (2), the system analyzes the dynamics of the embryo's 3-D motion and uses the Kalman filter to optimize the tracked results.

With the system dynamics modeled, the changes of embryo state in the VSs can be described by choosing the  $xyz$  positions and velocities as the state variables

$$X_k = AX_{k-1} + w_k, \quad (5)$$

where  $A$  is the state-transition matrix,  $w_k$  represents the noises affecting the actual state of the embryo caused by the heterogeneous response of the individual embryos, and  $w_k$  is assumed to have a Gaussian distribution  $[N(0, Q_k)]$ .

The embryo's position is calculated according to

$$Z_k = HX_k + v_k, \quad (6)$$

where  $H$  is the output matrix and  $v_k$  is the measurement noise, which is also assumed to have a Gaussian distribution  $[N(0, R_k)]$ .  $R_k$  is chosen based on the estimate of how accurately the embryo's 3-D positions are detected by image processing.

Based on the dynamic model, an a priori estimate of the state is computed ( $X_{k|k-1} = AX_{k-1|k-1} + w_k$ ). The error covariance is denoted as  $P_{k|k-1}$ . The a priori estimate for this covariance at time  $k$  is then determined by

$$P_{k|k-1} = AP_{k-1|k-1}A^T + Q_k. \quad (7)$$

With the a priori estimate of the state  $X_{k|k-1}$  and the measurement  $Z_k$  (i.e., the detected embryo position from image processing), the real state of the embryo in the VS is optimized by

$$X_{k|k} = X_{k|k-1} + K(Z_k - HX_{k|k-1}), \quad (8)$$

where  $K$  is the Kalman gain and is given by

$$K = \frac{P_{k|k-1}H^T}{HP_{k|k-1}H^T + R_k}. \quad (9)$$

With the optimized embryo 3-D position ( $X_{k|k}$ ), the robotic system controls the micropipette tip to retrieve the embryo out of the solutions via controlled aspiration [17]. A biological advantage of the embryo detection algorithm is that it enables the system to determine the optimized processing time based on measuring the volume change of an embryo (i.e., individualized timing, which is not possible to achieve in manual operation). In the VS, the embryos shrink in the beginning due to osmotic pressure. Then they re-expand to equilibrate with the VS. Since the cryoprotectant in the VS is toxic, the equilibration with the VS should be avoided [18]. Therefore, the robotic system retrieves and transfers the embryo out of the VS once its minimum volume is reached, according to the 3-D tracking results.

### Placing Embryo on Vitrification Straw

After washing the embryos in the ES and the VS under controlled timing, the vitrified embryos need to be placed on a vitrification straw tip. In this step, the excess medium must be removed from the vitrified embryo to ensure a high cooling rate in the liquid nitrogen. After detecting contact of the micropipette tip and the straw surface, the system dispenses the embryo with a relatively large volume of the VS solution onto the straw. The system then moves the micropipette tip on the straw surface away from the initial dispensing location to form a thin VS film [Figure 5(a)]. The robotic system controls the motorized syringe to aspirate the VS until the volume of the embryo droplet stops changing [Figure 5(b)]. When medium is aspirated into the micropipette, friction force acts on the embryo to keep it in the original place. To achieve this, the fluid speed from micropipette aspiration must be well controlled.

As shown in Figure 5(c), the embryo is also acted on by the drag force ( $F_d$ ) generated by micropipette aspiration flow

$$F_d = \frac{1}{2}\rho v^2 C_d A, \quad (10)$$

where  $\rho$  is the fluid density,  $v$  is the fluid velocity controlled by the motorized syringe,  $A$  is the cross-sectional area, and  $C_d$  is the drag coefficient. If the drag force is too large, the embryo can be undesirably moved together with the fluid into the micropipette. To keep the embryo in place on the straw, the drag force must be smaller than the friction force (i.e.,  $F_d < f = \mu mg$ ). Therefore, the aspiration flow rate should be below a threshold value. It was determined experimentally that the critical aspiration flow rate  $v$  must be controlled to be lower than 240  $\mu\text{m/s}$ . Below this threshold value, the minimum volume can be

achieved reliably. After removing the excess medium from around the embryo, the straw is plunged into liquid nitrogen for freezing. The vitrification straw is then sealed with a plastic cap and put in a liquid nitrogen tank for preservation.

## Results and Discussion

In the experiments, mouse embryos were gathered from the Canadian Mouse Mutant Repository in the Toronto Centre for Phenogenomics (Toronto, Ontario). Embryos were produced by superovulating a female and collected ~1.5–2.5 days after conception, which corresponds to the embryos being in the with KSOM medium (EMD Millipore, Billerica, United States) in a 35-mm Petri dish and covered with mineral oil to prevent evaporation.

The VS typically contains antifreezing agents or cryoprotectants such as DMSO, small molecular-sized glycols (e.g., ethylene glycol), or sucrose. In our experiments, the VS was made by diluting DMSO in KSOM medium at 20% concentration. The ES was at half the concentration of the VS (i.e., 10% DMSO). A multiwell plate (Repro Plate, Kitazato Corporation) was loaded with the ES and the VS for embryo washing. A standard vitrification straw (Cryotop, Kitazato Corporation) was used as the physical carrier to freeze embryos in liquid nitrogen. All vitrification experiments followed the Kitazato protocol by washing embryos in the ES and the VS for 12 min and 90 s, respectively. The robotic system can be readily reprogrammed to implement other vitrification protocols.

## System Performance

The system throughput was evaluated by processing the mouse embryos at the two-, four-, and eight-cell stages. The capability of automated pick and place of single embryos enabled the robotic system to perform vitrification of multiple embryos in an

optimally scheduled sequence. Since embryo equilibration in the ES costs minutes, after the first embryo was dispensed into the ES for equilibration, the robotic system moved back to the culture dish to pick up the next embryo and place it into the ES of another bath. Repeating this step to process six embryos in the ES, the system then retrieved the equilibrated embryos from the ES and washed them in the VS one by one, again following a prescheduled sequence. As a result, the system was able to process six embryos within 24 min. In comparison, in manual implementation of the same vitrification protocol, it was only possible to process two embryos in the same time period, and the operator was fully occupied in the process.

The success rate was also quantitatively evaluated. An experiment was defined to be successful when the system successfully processed the embryo within the given period of time for each step of a vitrification protocol. Manual vitrification experiments were also performed by three operators. The experimental results showed that the robotically vitrified group had a significantly higher success rate than the manual group (90% versus 83.3%, shown in Table 1). In manual vitrification, embryos could easily escape from operators' monitoring when they floated upward in the VS, which was the major cause of failure. Embryo loss was effectively avoided by the system's capability of 3-D embryo tracking in RoboVetri. However, failure in RoboVetri arose when an embryo floated in the VS solution and happened to drift into blind regions of the multiwell plate. The Repro Plate used in the experiments has inclined sidewalls that produce a dark blind region. Multiwell plates with vertical sidewalls can help reduce blind regions and, hence, system failure.

## Embryo Volume Measurement

In RoboVetri, the system is able to track embryos in 3-D space and monitor their volume change in real time for analyzing each individual embryo's response to the VSs. Figure 6 shows the tracked embryo position and the volume change of three different embryos in the VS, measured by the robotic system. When washed in the VS, the embryos first experience a dehydration stage in which water molecules are drawn out of the cell, causing the embryo to shrink. When the embryo reaches its minimum volume, the toxic cryoprotectant solutes (e.g., DMSO) start to penetrate the cell membrane. The embryo ideally should be transferred out of the VS at its minimum volume.

The experimental results summarized in Figure 6(b) demonstrate that the embryos reach their minimum volume in the VS at different time points. This suggests heterogeneity in embryo dehydration timing even in the same VS. All existing vitrification protocols stipulate a fixed washing time for all embryos because measuring the individual embryo's volume

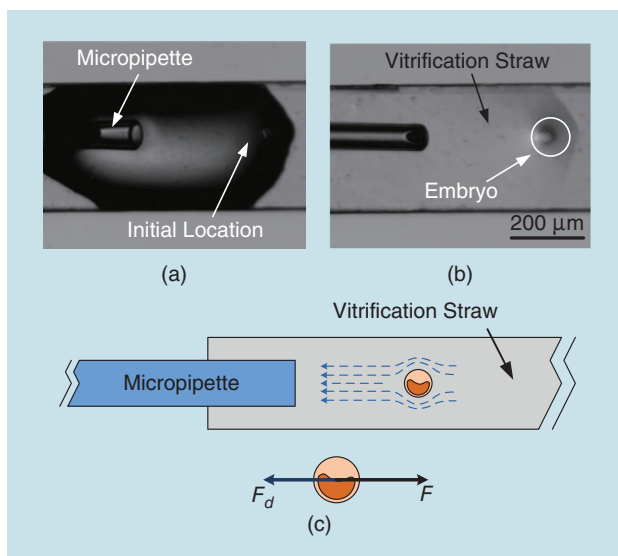


**Figure 5.** A processed embryo placed on the vitrification straw tip. (a) An embryo is deposited onto the straw by dispensing the VS medium out of the micropipette. (b) The excess medium removed by micropipette aspiration under a threshold flow rate to keep the embryo in place. (c) The schematic showing the embryo dynamics during micropipette aspiration.

**Table 1. Embryo vitrification experimental results.**

Method	Success Rate	Survival Rate	Development Rate
Control	N/A	100% (15/15)	93.3% (14/15)
Manual	83.3% (15/18)	73.3% (11/15)	90.9% (10/11)
Robotic	90% (18/20)	88.9% (16/18)	93.8% (15/16)

change is not feasible to achieve by human operators. In contrast, the robotic system is capable of measuring an embryo's volume throughout the vitrification process and is able to retrieve each embryo from the VS at its minimum volume point. Therefore, the toxic effects from the cryoprotectant solute (i.e., DMSO) can be minimized as the embryo is taken out of the VS when embryo dehydration has just ended.

### Post-Freezing Survival and Development Rates

The survival and development rates were defined to quantify the robotic system's performance. Survivability was measured by examining the morphology of the embryo before and after freezing, as commonly performed in the literature (see [19]). Embryos were considered unhealthy/dead if they had an abnormal shape, membrane damage, leakage of cellular content, or degeneration of their cytoplasm.

The development rate was determined by culturing the surviving embryos for an additional 24 h after thawing (Figure 7). If the cell number within the embryo increased, or if the embryo developed to the blastocyst stage, it was counted as developed. Control samples of nonvitrified embryos were also cultured to identify the base development rate of the mouse embryo population. Only embryos that had a healthy morphology after freezing were cultured following similar procedures to other vitrification studies [20].

The experimental results are summarized in Table 1. The robotically vitrified group had higher survival (88.9% versus 73.3%) and development rates (93.8% versus 90.9%) than the manually vitrified group. The higher survival and development rates produced by RoboVitri can be attributed to the optimized processing time achieved by the system through monitoring embryo volume changes in the VS. The ability of the system to effectively remove excess medium from around vitrified embryos on the straw (i.e., minimum volume vitrification for a higher cooling rate when freezing in liquid nitrogen) could also have enabled the robotic system to achieve higher embryo survival and development rates.

### Discussion

Vitrification is an essential technique in IVF for preserving oocytes and embryos. A number of different the VSs and protocols (e.g., Kitazato, Origio, and Irvine) have been developed and are commercially available. All of these protocols require multiple steps of embryo washing in different types of the VSs. With the automated capability, our robotic system can be programmed to test, optimize, and compare different vitrification protocols.

Besides embryo vitrification, oocyte vitrification is also important in IVF practice for preserving female fertility for future use. Oocyte vitrification requires more steps than embryo vitrification. For example, in the Kitazato protocol, oocyte vitrification involves three ES steps and two VS steps, whereas embryo vitrification only has one ES and VS step. The RoboVitri system can also be programmed to complete oocyte vitrification by simply repeating more washing steps because of its capability of automated pick and place and stringent time control.

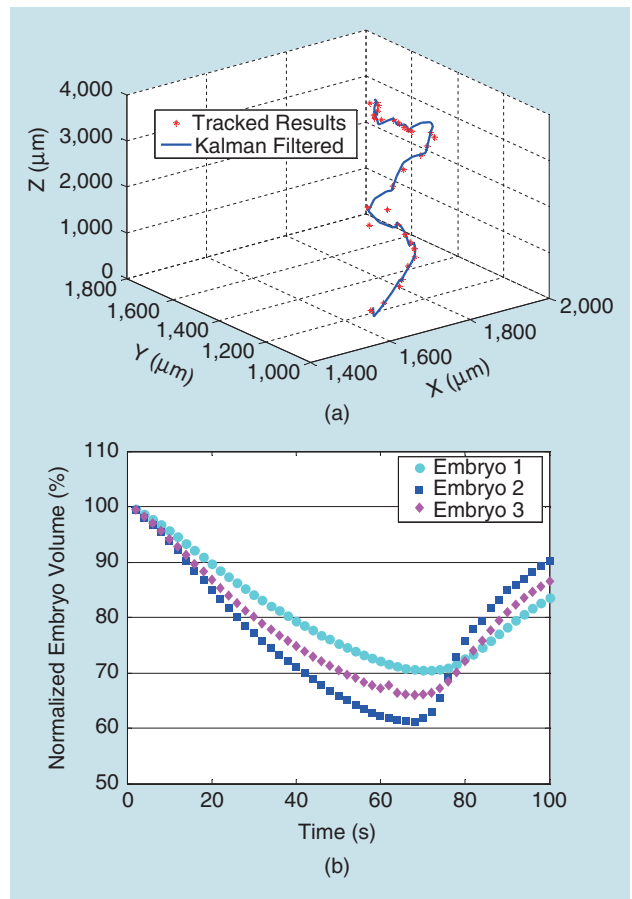


**Figure 6.** The 3-D-tracking results: (a) the z position change of a tracked embryo and (b) the volume change of three embryos in the same VS measured by the robotic system.

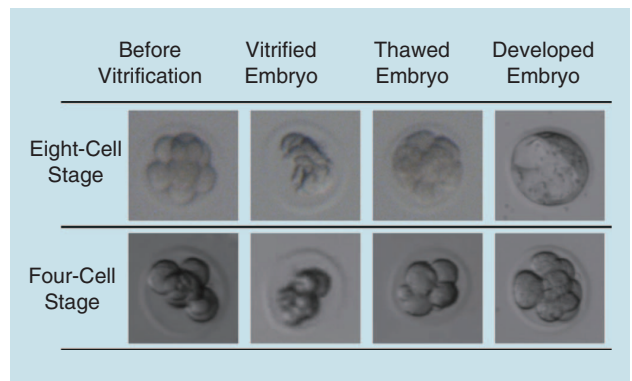


**Figure 7.** Example embryo images before and after vitrification.

Robotic cell manipulation relieves the human operator from tedious vitrification steps and eliminates manual operation-caused errors and inconsistencies. It also offers unparalleled timing control and the ability to leave a minimal volume of solution on vitrification straws. Automation also enables the system to process multiple oocytes/embryos with high efficiency. Efforts will continue to develop the system into an ideal tool for standardizing oocyte/embryo vitrification in IVF clinics and to achieve improved cryopreservation outcomes.

## Conclusion

This article presented an automated RoboVetri system capable of processing embryos with different the VSs. The system is integrated with two contact detection methods to determine the relative  $z$  position of the micropipette tip relative to embryos and vitrification straw tips. A 3-D embryo-tracking technique was developed to prevent embryo loss during multiple washing steps and achieve vision-guided embryo transfer. The 3-D embryo-tracking technique also enables the system to monitor real-time embryo volume changes in the VS, permitting individualized time control for each embryo. In the step of placing an embryo onto the vitrification straw tip, excess medium was automatically aspirated away from the vitrified embryo to obtain a high cooling rate. With these technical capabilities, the robotic system successfully achieved a high throughput and improved post-freezing survival and development rates compared to manual vitrification.

## Acknowledgments

We would like to acknowledge financial support from the University of Toronto, the Natural Sciences and Engineering Research Council of Canada (NSERC), the Canada Research Chairs Program, and the Shanghai Municipal Science and Technology Commission Project (Grant 14JC1491500).

## References

- [1] G. Vajta and M. Kuwayama, "Improving cryopreservation systems," *Theriogenology*, vol. 65, no. 1, pp. 236–244, Jan. 2006.
- [2] U.-B. Wennerholm, V. Söderström-Anttila, C. Bergh, K. Aittomäki, J. Hazekamp, K.-G. Nygren, A. Selbing, and A. Loft, "Children born after cryopreservation of embryos or oocytes: A systematic review of outcome data," *Hum. Reprod.*, vol. 24, no. 9, pp. 2158–2172, Sept. 2009.
- [3] K. E. Loutradi, E. M. Kolibianakis, C. A. Venetis, E. G. Papanikolaou, G. Pados, I. Bontis, and B. C. Tarlatzis, "Cryopreservation of human embryos by vitrification or slow freezing: A systematic review and meta-analysis," *Fertil. Steril.*, vol. 90, no. 1, pp. 186–193, July 2008.
- [4] W. F. Rall and G. M. Fahy, "Ice-free cryopreservation of mouse embryos at 196 degrees C by vitrification," *Nature*, vol. 313, no. 6003, pp. 573–575, 1985.
- [5] G. Vajta and Z. P. Nagy, "Are programmable freezers still needed in the embryo laboratory? Review on vitrification," *Reprod. Biomed. Online*, vol. 12, no. 6, pp. 779–796, Jan. 2006.
- [6] M. Kasai, J. H. Komi, A. Takakamo, H. Tsudera, T. Sakurai, and T. Machida, "A simple method for mouse embryo cryopreservation in a low toxicity vitrification solution, without appreciable loss of viability," *J. Reprod. Fertil.*, vol. 89, no. 1, pp. 91–97, 1990.
- [7] M. Kuwayama, "Highly efficient vitrification for cryopreservation of human oocytes and embryos: The Cryotop method," *Theriogenology*, vol. 67, no. 1, pp. 73–80, Jan. 2007.
- [8] K. Viigipuu and P. Kallio, "Microinjection of living adherent cells by using a semi-automatic microinjection system," *Altern. Lab. Animals*, vol. 32, no. 4, pp. 417–423, Oct. 2004.
- [9] X. Li, C. C. Cheah, S. Hu, and D. Sun, "Dynamic trapping and manipulation of biological cells with optical tweezers," *Automatica*, vol. 49, no. 6, pp. 1614–1625, June 2013.
- [10] A. Pillarsetti, M. Pekarev, A. D. Brooks, and J. P. Desai, "Evaluating the effect of force feedback in cell injection," *IEEE Trans. Autom. Sci. Eng.*, vol. 4, no. 3, pp. 322–331, 2007.
- [11] J. Liu, V. Siragam, J. Chen, M. D. Fridman, R. M. Hamilton, and Y. Sun, "High-throughput measurement of gap junctional intercellular

- communication," *Amer. J. Physiol.-Heart Circul.*, vol. 306, no. 12, pp. H1708–H1713, 2014.
- [12] Z. Lu, X. Zhang, C. Leung, N. Esfandiari, R. F. Casper, and Y. Sun, "Robotic ICSI (intracytoplasmic sperm injection)," *IEEE Trans. Biomed. Eng.*, vol. 58, no. 7, pp. 2102–2108, July 2011.
  - [13] Y. S. Heo, H.-J. Lee, B. A. Hassell, D. Irimia, T. L. Toth, H. Elmoazzen, and M. Toner, "Controlled loading of cryoprotectants (CPAs) to oocyte with linear and complex CPA profiles on a microfluidic platform," *Lab chip*, vol. 11, no. 20, pp. 3530–3537, Oct. 2011.
  - [14] D. G. Pyne, J. Liu, M. Abdelgawad, and Y. Sun, "Digital microfluidic processing of mammalian embryos for vitrification," *PLoS ONE*, vol. 9, no. 9, p. e108128, Sept. 2014.
  - [15] J. Liu, Z. Gong, K. Tang, Z. Lu, C. Ru, J. Luo, S. Xie, and Y. Sun, "Locating end-effector tips in robotic micromanipulation," *IEEE Trans. Robot.*, vol. 30, no. 99, pp. 1–6, 2013.
  - [16] S. F. Mullen, M. Li, Y. Li, Z.-J. Chen, and J. K. Critser, "Human oocyte vitrification: The permeability of metaphase II oocytes to water and ethylene glycol and the appliance toward vitrification," *Fertil. Steril.*, vol. 89, no. 6, pp. 1812–1825, June 2008.
  - [17] X. P. Zhang, C. Leung, Z. Lu, N. Esfandiari, R. F. Casper, and Y. Sun, "Controlled aspiration and positioning of biological cells in a micropipette," *IEEE Trans. Biomed. Eng.*, vol. 59, no. 4, pp. 1032–1040, Apr. 2012.
  - [18] M. H. Johnson and S. J. Pickering, "The effect of dimethylsulphoxide on the microtubular system of the mouse oocyte," *Development*, vol. 100, no. 2, pp. 313–324, June 1987.
  - [19] A. Dhali, V. M. Anchamparuthy, S. P. Butler, R. E. Pearson, I. K. Mullarky, and F. C. Gwazdauskas, "Effect of droplet vitrification on development competence, actin cytoskeletal integrity and gene expression in in vitro cultured mouse embryos," *Theriogenology*, vol. 71, no. 9, pp. 1408–1416, June 2009.
  - [20] J. Zhang, J. Cui, X. Ling, X. Li, Y. Peng, X. Guo, B. C. Heng, and G. Q. Tong, "Vitrification of mouse embryos at 2-cell, 4-cell and 8-cell stages by cryotop method," *J. Assist. Reprod. Genet.*, vol. 26, nos. 11–12, pp. 621–628, 2009.

**Jun Liu**, University of Toronto, Ontario, Canada. E-mail: [ljun@mie.utoronto.ca](mailto:ljun@mie.utoronto.ca).

**Chaoyang Shi**, University of Toronto, Ontario, Canada. E-mail: [cysshi@mie.utoronto.ca](mailto:cysshi@mie.utoronto.ca).

**Jun Wen**, University of Toronto, Ontario, Canada. E-mail: [dan.wen@mail.utoronto.ca](mailto:dan.wen@mail.utoronto.ca).

**Derek Pyne**, University of Toronto, Ontario, Canada. E-mail: [dpyne@mie.utoronto.ca](mailto:dpyne@mie.utoronto.ca).

**Haijiao Liu**, University of Toronto, Ontario, Canada. E-mail: [haijiao.liu@utoronto.ca](mailto:haijiao.liu@utoronto.ca).

**Changhai Ru**, Harbin Engineering University, China. E-mail: [rchai@gmail.com](mailto:rchai@gmail.com).

**Jun Luo**, Shanghai University, China. E-mail: [luojun@shu.edu.cn](mailto:luojun@shu.edu.cn).

**Shaorong Xie**, Shanghai University, China. E-mail: [srxie@shu.edu.cn](mailto:srxie@shu.edu.cn), [srxie@263.net](mailto:srxie@263.net).

**Yu Sun**, University of Toronto, Ontario, Canada; Harbin Engineering University, China; Shanghai University, China. E-mail: [sun@mie.utoronto.ca](mailto:sun@mie.utoronto.ca).

